International Journal of Modern Physics A
Vol. 38, Nos. 4 & 5 (2023) 2350026 (14 pages)

DOI: 10.1142/S0217751X23500264

World Scientific
www.worldscientific.com

The eye of the storm: Optical properties

Bakhtiyor Narzilloev[*,†,‡,§,¶,††] and Bobomurat Ahmedov[‡,‖,**,§§]

[*]*New Uzbekistan University,*
Mustaqillik Avenue 54,
Tashkent 100007, Uzbekistan

[†]*Akfa University, Milliy Bog' Street 264,*
Tashkent 111221, Uzbekistan

[‡]*Ulugh Beg Astronomical Institute,*
Astronomy Street 33,
Tashkent 100052, Uzbekistan

[§]*Samarkand State University,*
University Avenue 15,
Samarkand 140104, Uzbekistan

[¶]*Tashkent Institute of Irrigation*
and Agricultural Mechanization Engineers,
Kori Niyoziy, 39, Tashkent 100000, Uzbekistan

[‖]*National University of Uzbekistan,*
Tashkent 100174, Uzbekistan

[**]*Institute of Fundamental and Applied Research,*
National Research University TIIAME,
Kori Niyoziy 39, Tashkent 100000, Uzbekistan
[††]*nbakhtiyor18@fudan.edu.cn*
[§§]*ahmedov@astrin.uz*

Received 13 January 2023
Revised 20 February 2023
Accepted 23 February 2023
Published 5 April 2023

Investigation of the optical properties of a black hole described by the so-called "eye of the storm" space–time has been the main aim of the work. Such a space–time is regular and recovers the Minkowski space–time at asymptotical infinity due to the effect of the so-called "suppression parameter" involved in the metric. It has been shown that an increase in the suppression parameter reduces the inclination angle of photons in the close regions around a black hole due to gravitational lensing. Investigation of the photon motion has also shown that bigger values of this parameter reduce the photon sphere radius as well. It has been also detected that the shape of a black hole shadow is affected in the presence of the suppression parameter and the bigger values of this parameter twist the shape of a shadow stronger. Lastly, it has been demonstrated that the average shadow radius is bigger for smaller suppression parameters and the distortion of the shape of shadow from a circle is bigger for bigger suppression parameters and bigger spin of a black hole.

[§§]Corresponding author.

Keywords: General relativity; modified gravity theories; black holes; photon motion; shadow of a black hole.

PACS numbers: 04.20.q, 04.50.+h, 04.70.s, 04.70.Bw, 04.50.−h

1. Introduction

Theoretical predictions on the properties of astrophysical compact objects can be probed through recent experimental observations. The detection of gravitational waves by the LIGO/Virgo collaboration from merger events in close binaries[1–3] and the first images of the M87* and SgrA* black holes (BHs) by the Event Horizon Telescope (EHT)[4–9] can be used to test the gravity theories in strong field regime. Combined with the planned next-generation ground-based observatories,[10] it may enable the delineation between candidate space–times based on their astrophysical signature. The extraction of astrophysical observables for nonsingular candidate geometries has been extensively performed in the recent literature.[11–26]

Regular BHs (RBHs) represent a subset of the nonsingular geometries first introduced by Bardeen in the pioneering study,[27] where orthonormal curvature tensor components and Riemann curvature invariants are regularized through enforcing global finiteness. RBHs have been extensively explored for both spherical and axial symmetry cases in the literature.[13–16,21,22,27–51] Space–time properties of several BH solutions have been tested in our previous research works including regular solutions as well.[52–62] Our aim here is to study photon motion around a rotating RBH with an asymptotically Minkowski core proposed by Ghosh[38] and develop its optical features. The stationary axial symmetric space–time is constructed as a deviation of the Kerr one and possesses the nontrivial Killing tensor, full "Killing tower"[63] of principal tensor and Killing–Yano tensor. A fourth constant of the motion is called an associated Carter constant[64,65] giving the integrable geodesic equations of motion for test particles (i.e. separability of the Hamilton–Jacobi equation).

Here, we study photon motion and related optical phenomena such as gravitational lensing (GL) and BH shadow in the RBH space–time which is labeled as the "eye of the storm" (eos) space–time.[66] The effects of the "suppression parameter" related to eos space–time will be explored in detail. In the recent study,[67] the shadow cast around a BH described by the studied space–time metric was explored to explain observed images of M87* and SgrA*. However, our work utilizes a different method outlined in Ref. 68 to simulate images of the BH's shadow, resulting in different observables R_s and δ_s compared to those found in Ref. 67. In addition, we examine here the properties of singularity, event horizon, ISCO, photon sphere and GL.

This paper has the following structure. Section 2 is devoted to the space–time structure of the eos BH. The GL in the space–time of eos BH is studied in Sec. 3. The shadow of eos BH is explored in Sec. 4. The main results are summarized in Sec. 5. The signature of the space–time is $(-,+,+,+)$, the geometrized units where $G = c = 1$ are selected, and Greek indices run through $0, 1, 2, 3$.

2. Brief Introduction of the Eos BH

The eos space–time describing regular and rotating BHs is given by the following metric[66]:

$$ds^2 = \frac{\Sigma}{\Delta}dr^2 + \Sigma d\theta^2 - \frac{\Delta}{\Sigma}(dt - a\sin^2\theta d\phi)^2 + \frac{\sin^2\theta}{\Sigma}[(r^2 + a^2)d\phi - adt]^2, \quad (1)$$

where

$$\Sigma = r^2 + a^2\cos^2\theta, \quad \Delta = r^2 + a^2 - 2Mre^{-l/r}, \quad (2)$$

with parameter l that is called as suppression parameter. Here, one may define the mass function as $m(r) = Me^{-l/r}$. It is easy to check that in the case $l = 0$ the given space–time recovers the Kerr metric. From the equation, $\Delta = 0$ one can find the relation between the event horizon radius and the space–time parameters as shown in Fig. 1. One can see that increase of both space–time parameters l and a reduces the size of the event horizon.

One can also check the regularity of the given space–time by calculating the Kretschmann scalar defined as $\mathcal{K} = R_{\alpha\beta\mu\nu}R^{\alpha\beta\mu\nu}$ which has the following simple form when $\theta = \pi/2$:

$$\mathcal{K} = \frac{4m^2e^{-\frac{2l}{r}}(l^4 - 8l^3r + 24l^2r^2 - 24lr^3 + 12r^4)}{r^{10}}, \quad (3)$$

from which one can see that in the case of $r \to 0$ the exponential part approaches zero faster than the denominator so the curvature in the center tends to zero as well.

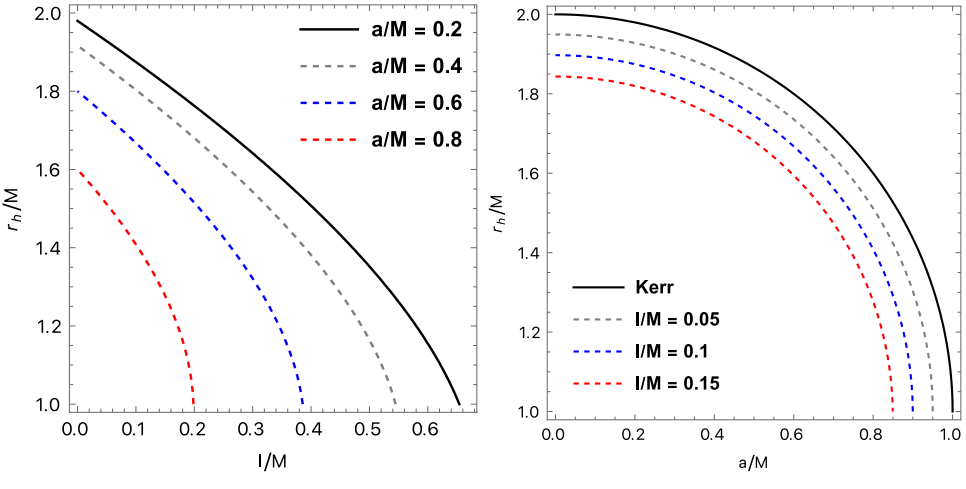

Fig. 1. Impact of the space–time parameters on the event horizon radius of the eos BH. The left panel demonstrates the dependence of the radius of BH from the suppression parameter for the different values of BH spin. The right panel demonstrates the dependence of the radius of BH from the BH spin for the different values of suppression parameter.

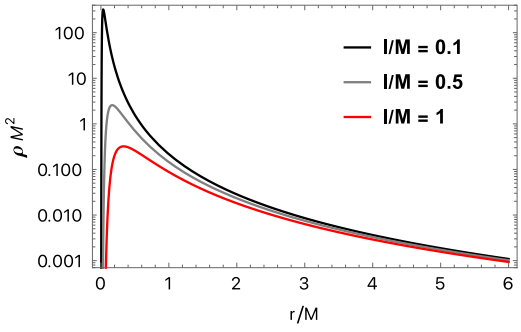

Fig. 2. Effect of the suppression parameter on the mass density parameter of the eos BH and its radial dependence.

One can introduce the mass density parameter by simply defining it as

$$\rho(r) = \frac{m(r)}{\frac{4}{3}\pi r^3}.$$

The distribution of mass can be illustrated by this function as presented in Fig. 2. It can be seen that the mass density becomes bigger for smaller values of the suppression parameter l. Since we plan to investigate the optical properties of a BH described by eos space–time it is more beneficial to take the mass density to be large which is common for all compact astrophysical objects. For this reason, hereafter, in the work we take the average value of the suppression parameter to be around $l/M \sim 0.1$.

3. Photon Geodesics and GL

We plan to discuss the GL in the space–time of eos BH based on the analysis of the motion of photons.

3.1. *Photon motion*

The Hamilton–Jacobi equation of motion

$$\frac{\partial S}{\partial \lambda} = -\frac{1}{2} g^{\alpha\beta} \frac{\partial S}{\partial x^\alpha} \frac{\partial S}{\partial x^\beta}, \tag{4}$$

can be applied to investigate photon geodesics, where λ is the affine parameter. In the axially symmetric space–time of the eos BH, the action can be written in the following separable form:

$$S = -\mathcal{E}t + \mathcal{L}\phi + S(r, \theta), \tag{5}$$

where $\mathcal{E}$ is the conserved energy and $\mathcal{L}$ is the angular momentum of photon. The Hamilton–Jacobi equation of motion is separable in the eos BH space–time and the

components of the four-velocity take the following form:

$$\begin{aligned}
\dot{t} &= \frac{(a^2+r^2)(\mathcal{E}(a^2+r^2)-a\mathcal{L})+\Delta\chi\csc^2\theta(\mathcal{L}-\chi\mathcal{E})}{\Delta\Sigma},\\
\dot{\phi} &= \frac{a(\mathcal{E}(a^2+r^2)-a\mathcal{L})+\Delta\csc^2\theta(\mathcal{L}-\chi\mathcal{E})}{\Delta\Sigma},\\
f(r) = \dot{r} &= \frac{\sqrt{(\mathcal{E}(a^2+r^2)-a\mathcal{L})^2-\Delta\mathcal{K}}}{\Sigma},\\
\dot{\theta} &= \frac{\sqrt{\mathcal{K}-(\mathcal{L}\csc\theta-a\mathcal{E}\sin\theta)^2}}{\Sigma},
\end{aligned} \tag{6}$$

where $\mathcal{K}$ is the Carter constant, and notation $\chi = a\sin^2\theta$ is introduced for convenience.

3.2. *Gravitational lensing*

The gravitational field of the central eos BH causes the lensing of the passing photons. One can assume that a photon is in the equatorial plane of the eos BH and traveling from asymptotic infinity with impact parameter $b = \mathcal{L}/\mathcal{E}$ and then it is traveling back to infinity. The relationship between the radius of the closest approaches r_0 and the impact parameter is obtained from the third equation in the system (6) using the condition $\dot{r} = 0$. For the selected values of the space–time parameters, the relation between r_0 and b is presented in Fig. 3. In the left panel of Fig. 3, the lines are for the different values of the suppression parameter when the BH

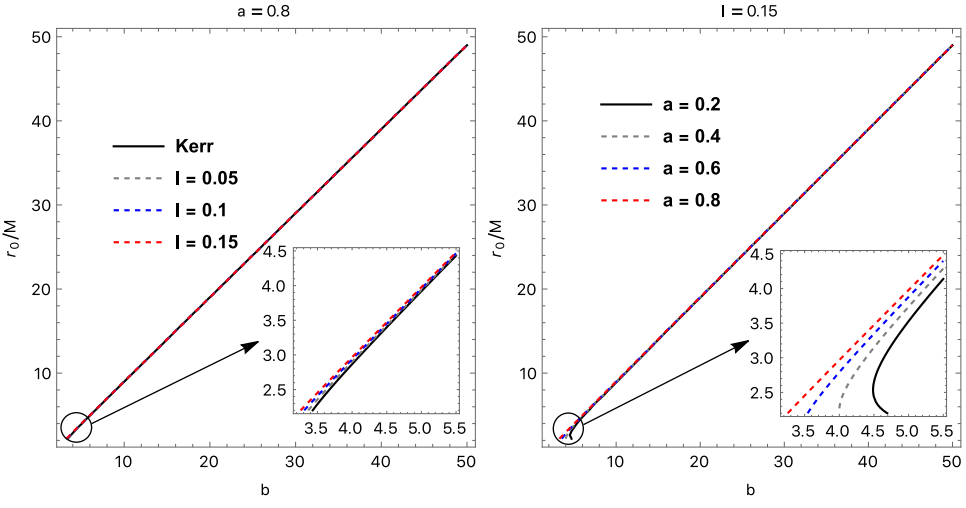

Fig. 3. Change of the radius of the closest approach of a photon to the central BH with the change of the impact parameter. In the left panel, the lines are for the different values of the suppression parameter when the BH spin is fixed. The right panel is for the fixed values of the BH spin for the different values of the suppression parameter.

spin is fixed. In the right panel of Fig. 3, the lines are for the different values of BH spin when the suppression parameter is fixed. From the plots, one can notice that the radius of the closest approach tends to the impact parameter for bigger distances as it should be i.e. when the photon is fired from bigger distances from the central BH, the inclination becomes smaller which in turn makes the difference between the radius of the closest approach and the impact parameter smaller.

The dependence between the radial coordinate r and the angle ϕ

$$\frac{d\phi}{dr} = \frac{a(\mathcal{E}(a^2+r^2) - a\mathcal{L}) + \Delta \csc^2\theta(\mathcal{L} - \chi\mathcal{E})}{\Delta\sqrt{(\mathcal{E}(a^2+r^2) - a\mathcal{L})^2 - \Delta\mathcal{K}}}, \tag{7}$$

is obtained from the second and third expressions in (6) at the equatorial plane ($\theta = \pi/2$).

A new variable being inversely proportional to the radial coordinate as $u = 1/r$ is introduced in order to simplify the calculations. The expression above can be written through the new variable as

$$\frac{d\phi}{du} = -\frac{d\phi}{dr}\frac{1}{u^2}.$$

Integration of this expression provides the dependence between the bending angle of the photon and the inverse of the radius of the closest approach $u_0 = 1/r_0$ for different values of the space–time parameters as

$$\delta = 2\int_0^{u_0} \frac{d\phi}{du} du - \pi. \tag{8}$$

It is not easy to evaluate the integral in analytical form. However, it can be integrated numerically for getting the dependence as presented in Fig. 4. u_0 is inversely proportional to the radius of the closest approach and consequently, with the increase of the values of this parameter, the photon approaches closer to the central BH. The first plot of Fig. 4 indicates that the bending angle becomes smaller for

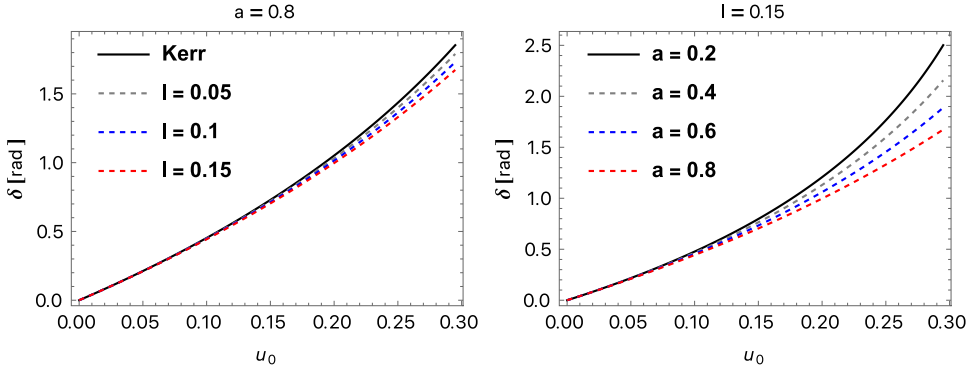

Fig. 4. The dependence of the bending angle of photons δ from the parameter of closest approach u_0 for the different values of space–time parameters.

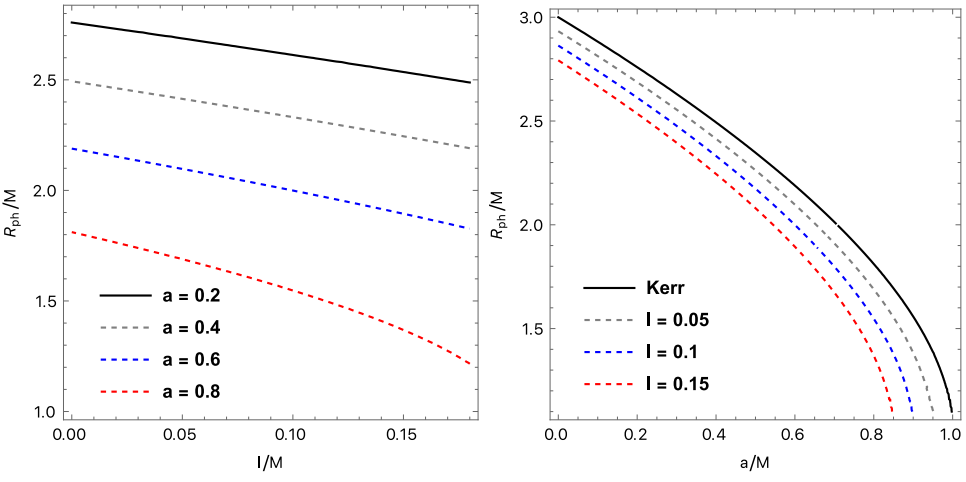

Fig. 5. Dependence of the photon sphere radius on the suppression parameter of the eos BH (the left panel) and on the eos BH spin (the right panel).

bigger values of the suppression parameter. However, this effect is dominant in the close environment of the central BH while at the bigger distances, the influence of the suppression parameter is negligible. The right panel represents the effect of the BH spin parameter on the bending angle of the photon which has a similar effect as the effect of the suppression parameter with the more substantial impact at the close environment of the central gravitating object.

The knowledge of the dependence of the photon sphere on the space–time parameters is crucial to study the BH shadow. It can be achieved through funding solutions of equations defined by the following conditions:

$$f(r) = 0, \tag{9}$$

$$f'(r) = 0, \tag{10}$$

where the prime is introduced for the derivative on the radial coordinate r and the function $f(r)$ is governed by (6). Figure 5 represents the dependence of the photon sphere on the space–time parameters. One can observe from the comparison of the right plot to the left one (The left plot represents the decrease of the photon sphere radius with the increase of the spin of a BH.) that the increase of the suppression parameter of eos BH reduces the photon sphere radius and its rate is stronger when compared to the effect of the spin of a BH. However, a decrease in the inclination angle corresponds to a weaker gravitational effect on the photon and consequently increase in these two space–time parameters weakens the total gravitational field of the central BH.

One may conclude that the suppression parameter and BH spin both weaken the resulting gravitational attraction.

4. BH Shadow

In order to describe the shadow of the BH one may use the celestial coordinates defined as follows (see, for example, Ref. 68):

$$x = \lim_{r_0 \to \infty} \left(-r_0^2 \sin\theta_0 \frac{d\phi}{dr} \right), \tag{11}$$

and

$$y = \lim_{r_0 \to \infty} r_0^2 \frac{d\theta}{dr}. \tag{12}$$

The diagram in Fig. 6 illustrates the angular position θ_0 of the axis of rotation of a BH relative to an observer's line of sight, as well as the distance r_0 between the observer and the BH. The coordinates x and y in Fig. 6 indicate the location of the image points in relation to the equatorial plane and the axis of symmetry, respectively. By using the equations for $d\phi/dr$ and $d\theta/dr$ given in (6), one can derive the expressions for x and y for the space–time described by (1) as

$$x = -b_1 \csc\theta_0, \tag{13}$$

$$y = \pm \sqrt{b_2 - (b_1 \csc\theta_0 - a\sin\theta_0)^2}. \tag{14}$$

The impact parameters $b_1 = \mathcal{L}/\mathcal{E}$ and $b_2 = \mathcal{K}/\mathcal{E}^2$ in Eqs. (13) and (14) represent the characteristics of the general orbits around a BH. For a comprehensive calculation of these parameters for the Kerr space–time, readers can refer to Ref. 68. To determine

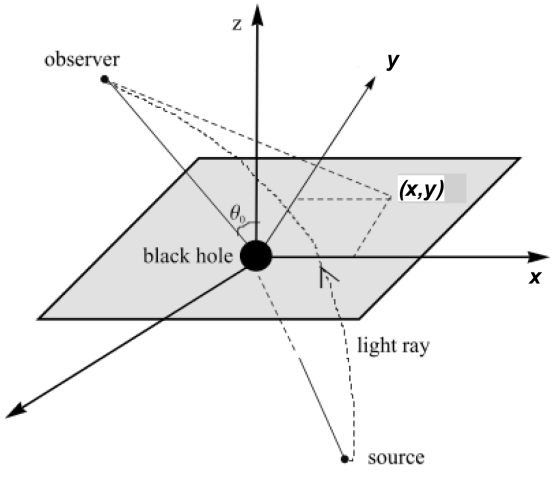

Fig. 6. The scheme of location of gravitational lens object between the astronomical illuminating source and a far observer. A far observer selects a reference coordinate system originating at the BH. At asymptotic infinity, the Boyer–Lindquist coordinates approach the Cartesian coordinate system. A far observer at infinity observes the BH as rotating around the z-axis along the selected reference frame. Here, the origin is joined with the observer along the line being orthogonal to the xy-plane. An incoming light ray defines a tangent vector as being responsible for a straight line crossing the xy-plane at the point (x, y).

these parameters, one can utilize the conditions $\dot{r} = 0 = \partial_r \dot{r}$, which result in the expressions provided as follows:

$$b_1 = -\frac{(a^2 + r^2)(lM + r^2 e^{l/r} + Mr) - 4Mr^3}{a(-lM + r^2 e^{l/r} - Mr)}, \tag{15}$$

$$b_2 = \frac{4r^4 e^{l/r}[(a^2 + r^2)e^{l/r} - 2Mr]}{[r(M - re^{l/r}) + lM]^2}. \tag{16}$$

To characterize the shape of the shadow of a rotating BH, two observables can be introduced. Three points on the border of the shadow, denoted as (A), (B) and (C) in Fig. 7, can be selected to define the radius of the BH shadow R_s. Point (C) corresponds to the unstable retrograde equatorial circular orbits that are observed by a distant observer. By measuring the deflection $D_{\rm cs}$, which is the difference between the left endpoints of the reference circle passing through the selected points and the image of the BH shadow's left endpoint, the dimensionless distortion parameter δ_s can be defined as $\delta_s = D_{\rm cs}/R_s$. These two observables, R_s and δ_s, can be utilized to characterize the shadow of rotating BHs.[69] When the distant observer is located on the equatorial plane, i.e. $\theta_0 = \pi/2$, the maximum gravitational effects on the shadow of the BH due to rotation can be observed. For the supermassive BH SgrA* at the center of our Galaxy, the inclination angle is also expected to be close to $\pi/2$ and consequently

$$x = -b_1, \tag{17}$$

$$y = \pm\sqrt{b_2 - (a - b_1)^2}. \tag{18}$$

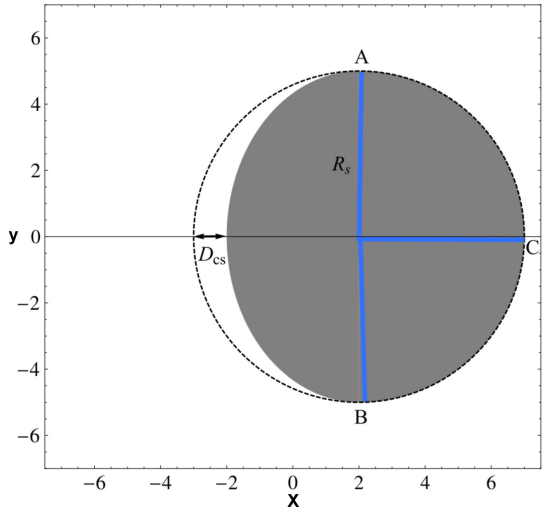

Fig. 7. The BH shadow radius R_s and the distortion parameter $D_{\rm cs}$ between the left endpoints of the circle and the apparent shape of a BH play a role of two observables describing BH shadow.[13]

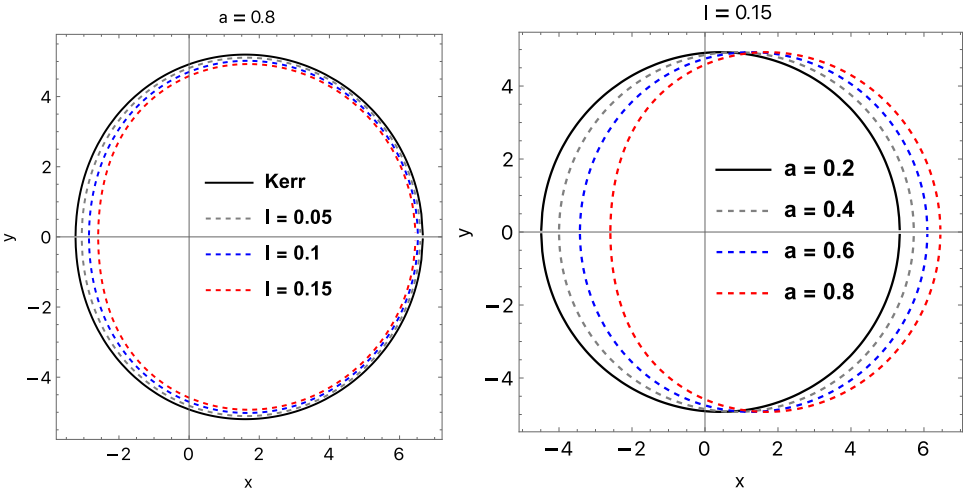

Fig. 8. The shape of the shadow of the eos BH observed at infinity for the different values of spin and suppression parameter of BH. Comparison of the two panels shows that the spin of BH is much more efficient to distort the eos BH shadow rather than the suppression parameter.

The shape of the shadow of the eos BH can be obtained based on the expressions for x and y. Figure 8 represents the shadows of eos BH. The shape and size of the shadow of eos BH for the different values of the suppression parameter l are demonstrated in the left plot of Fig. 8. One can observe that the increase of the suppression parameter shrinks the total area of the BH shadow and makes the BH shape more twisted. According to the right panel, the effect of the BH suppression parameter on the BH shadow is similar to the Kerr one i.e. it shifts the shadow to right (with respect to the observer) and twists the left side. It is observed that an increase in the suppression parameter weakens the total gravitational field around the BH and the BH shadow size is decreased accordingly.

The observable R_s of BH shadow is introduced as

$$R_s = \frac{(x_C - x_A)^2 + y_A^2}{2(x_C - x_A)}, \tag{19}$$

and the second observable δ_s of BH shadow is introduced as

$$\delta_s = \frac{D_{\rm cs}}{R_s}. \tag{20}$$

The left plot in Fig. 9 represents R_s and the right one is for δ_s for the selected values of the space–time parameters of the eos BH. One can observe from the left plot of Fig. 9 that the average radius of the BH shadow almost does not depend on the BH spin and is mostly affected by the BH suppression parameter. The increase of the suppression parameter weakens the gravitational field around the BH and consequently reduces the average radius of the BH shadow. The right plot demonstrates

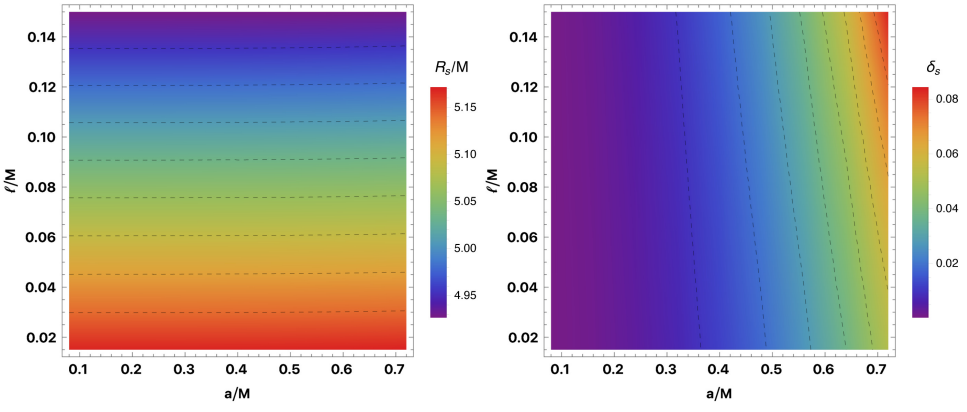

Fig. 9. The dependence of R_s and δ_s on the space–time parameters. The left panel indicates that the shadow size is very sensitive to the suppression parameter. The right panel represents that the deflection strongly depends on the BH spin.

that the distortion parameter which defines the distortion of the shape of the BH shadow from a circle is higher for a faster spin and a bigger suppression parameter. One can also notice that the effect of the spin on the distortion parameter is stronger compared to the effect of the suppression parameter.

5. Conclusion

In the work, the optical properties of eos BHs have been investigated. Investigation of the photon motion has shown that in the close distances increase of the suppression, the parameter increases the radius of the closest approach of photons to the central eos BH for the fixed impact parameter and in the far distances, the effect of this parameter is negligible. The effect of the spin is similar to the effect of the suppression parameter but in the close environment of a BH, the effect of the spin is considerably stronger than the effect of the suppression parameter. GL of photons in the space–time of eos BH has shown that a smaller bending angle corresponds to bigger values of the suppression parameter and only at close distances from the central BH such an effect is perceptible. The effect of the spin on the bending angle is also noticeable only in the close environment of a BH but considerably stronger than the effect of the suppression parameter again. Photon sphere radius decreases with the increase of both space–time parameters. Investigation of the shadow formed around eos BH has revealed that an increase in the suppression parameter makes the shadow size smaller and twists the shape stronger. The effect of the spin of a BH is similar to the Kerr BH. The average shadow radius is weakly dependent on the spin but the distortion of the shape from a circle is strongly dependent on the former. The suppression parameter has a stronger effect on the average radius of the shadow but a weaker effect on the distortion parameter compared to the effect of the spin of the eos BH.

Acknowledgment

This research is supported by Grants F-FA-2021-432 and MRB-2021-527 of the Uzbekistan Ministry for Innovative Development.

References

1. LIGO Scientific, VIRGO, KAGRA Collab. (R. Abbott *et al.*), arXiv:2111.03604 [astro-ph.CO].
2. LIGO Scientific, VIRGO, KAGRA Collab. (R. Abbott *et al.*), arXiv:2111.03606 [gr-qc].
3. LIGO Scientific, VIRGO, KAGRA Collab. (R. Abbott *et al.*), arXiv:2112.06861 [gr-qc].
4. Event Horizon Telescope Collab. (K. Akiyama *et al.*), *Astrophys. J. Lett.* **875**, **L1** (2019), https://doi.org/10.3847/2041-8213/ab0ec7, arXiv:1906.11238 [astro-ph.GA].
5. Event Horizon Telescope Collab. (K. Akiyama *et al.*), *Astrophys. J. Lett.* **875**, **L2** (2019), https://doi.org/10.3847/2041-8213/ab0c96, arXiv:1906.11239 [astro-ph.IM].
6. Event Horizon Telescope Collab. (K. Akiyama *et al.*), *Astrophys. J. Lett.* **875**, **L3** (2019), https://doi.org/10.3847/2041-8213/ab0c57, arXiv:1906.11240 [astro-ph.GA].
7. Event Horizon Telescope Collab. (K. Akiyama *et al.*), *Astrophys. J. Lett.* **930**, **L12** (2022), https://doi.org/10.3847/2041-8213/ac6674.
8. Event Horizon Telescope Collab. (K. Akiyama *et al.*), *Astrophys. J. Lett.* **930**, **L13** (2022), https://doi.org/10.3847/2041-8213/ac6675.
9. Event Horizon Telescope Collab. (K. Akiyama *et al.*), *Astrophys. J. Lett.* **930**, **L14** (2022), https://doi.org/10.3847/2041-8213/ac6429.
10. V. Kalogera *et al.*, arXiv:2111.06990 [gr-qc].
11. E. F. Eiroa and C. M. Sendra, *Class. Quantum Grav.* **28**, 085008 (2011), https://doi.org/10.1088/0264-9381/28/8/085008, arXiv:1011.2455 [gr-qc].
12. A. Flachi and J. P. S. Lemos, *Phys. Rev. D* **87**, 024034 (2013), https://doi.org/10.1103/PhysRevD.87.024034, arXiv:1211.6212 [gr-qc].
13. L. Amarilla, E. F. Eiroa and G. Giribet, *Phys. Rev. D* **81**, 124045 (2010), https://doi.org/10.1103/PhysRevD.81.124045.
14. R. Carballo-Rubio, F. Di Filippo, S. Liberati, C. Pacilio and M. Visser, *J. High Energy Phys.* **2018**, 023 (2018), https://doi.org/10.1007/JHEP07(2018)023, arXiv:1805.02675 [gr-qc].
15. R. Carballo-Rubio, F. Di Filippo, S. Liberati and M. Visser, *Class. Quantum Grav.* **37**, 14 (2020), https://doi.org/10.1088/1361-6382/ab8141, arXiv:1908.03261 [gr-qc].
16. R. Carballo-Rubio, F. Di Filippo, S. Liberati and M. Visser, *Phys. Rev. D* **101**, 084047 (2020), https://doi.org/10.1103/PhysRevD.101.084047, arXiv:1911.11200 [gr-qc].
17. D.-C. Dai and D. Stojkovic, *Phys. Rev. D* **100**, 083513 (2019), https://doi.org/10.1103/PhysRevD.100.083513, arXiv:1910.00429 [gr-qc].
18. J. G. Cramer, R. L. Forward, M. S. Morris, M. Visser, G. Benford and G. A. Landis, *Phys. Rev. D* **51**, 3117 (1995), https://doi.org/10.1103/PhysRevD.51.3117, arXiv:astro-ph/9409051.
19. J. H. Simonetti, M. J. Kavic, D. Minic, D. Stojkovic and D.-C. Dai, *Phys. Rev. D* **104**, **L081502** (2021), https://doi.org/10.1103/PhysRevD.104.L081502, arXiv:2007.12184 [gr-qc].
20. T. Berry, A. Simpson and M. Visser, *Universe* **7**, 2 (2020), https://doi.org/10.3390/universe7010002, arXiv:2008.13308 [gr-qc].
21. R. Carballo-Rubio, F. Di Filippo and S. Liberati, *Int. J. Mod. Phys. D* **30**, 2142024 (2021), https://doi.org/10.1142/S0218271821420244, arXiv:2106.01530 [gr-qc].

22. R. Carballo-Rubio, F. Di Filippo, S. Liberati and M. Visser, *J. High Energy Phys.* **2022**, 122 (2022), https://doi.org/10.1007/JHEP02(2022)122, arXiv:2111.03113 [gr-qc].
23. K. A. Bronnikov, R. A. Konoplya and T. D. Pappas, *Phys. Rev. D* **103**, 124062 (2021), https://doi.org/10.1103/PhysRevD.103.124062, arXiv:2102.10679 [gr-qc].
24. M. S. Churilova, R. A. Konoplya, Z. Stuchlik and A. Zhidenko, *J. Cosmol. Astropart. Phys.* **2021**, 010 (2021), https://doi.org/10.1088/1475-7516/2021/10/010, arXiv:2107.05977 [gr-qc].
25. C. Bambi and D. Stojkovic, *Universe* **7**, 136 (2021), https://doi.org/10.3390/universe7050136, arXiv:2105.00881 [gr-qc].
26. A. M. Simpson, *Universe* **7**, 418 (2021), https://doi.org/10.3390/universe7110418, arXiv:2109.11878 [gr-qc].
27. J. M. Bardeen, Non-singular general-relativistic gravitational collapse, in *Proc. Int. Conf. GR5*, Tbilisi (1968), p. 174.
28. E. Ayon-Beato and A. Garcia, *Phys. Lett. B* **493**, 149 (2000), https://doi.org/10.1016/S0370-2693(00)01125-4, arXiv:gr-qc/0009077.
29. S. A. Hayward, *Phys. Rev. Lett.* **96**, 031103 (2006), https://doi.org/10.1103/PhysRevLett.96.031103, arXiv:gr-qc/0506126.
30. K. A. Bronnikov and J. C. Fabris, *Phys. Rev. Lett.* **96**, 251101 (2006), https://doi.org/10.1103/PhysRevLett.96.251101, arXiv:gr-qc/0511109.
31. C. Bambi and L. Modesto, *Phys. Lett. B* **721**, 329 (2013), https://doi.org/10.1016/j.physletb.2013.03.025, arXiv:1302.6075 [gr-qc].
32. Z. Li and C. Bambi, *J. Cosmol. Astropart. Phys.* **2014**, 041 (2014), https://doi.org/10.1088/1475-7516/2014/01/041, arXiv:1309.1606 [gr-qc].
33. K. Jusufi and A. Övgün, *Phys. Rev. D* **97**, 024042 (2018), https://doi.org/10.1103/PhysRevD.97.024042, arXiv:1708.06725 [gr-qc].
34. K. Jusufi, M. Jamil, H. Chakrabarty, Q. Wu, C. Bambi and A. Wang, *Phys. Rev. D* **101**, 044035 (2020), https://doi.org/10.1103/PhysRevD.101.044035, arXiv:1911.07520 [gr-qc].
35. K. Jusufi, M. Azreg-Aïnou, M. Jamil, S.-W. Wei, Q. Wu and A. Wang, *Phys. Rev. D* **103**, 024013 (2021), https://doi.org/10.1103/PhysRevD.103.024013, arXiv:2008.08450 [gr-qc].
36. C. Herdeiro, E. Radu and H. Rúnarsson, *Class. Quantum Grav.* **33**, 154001 (2016), https://doi.org/10.1088/0264-9381/33/15/154001, arXiv:1603.02687 [gr-qc].
37. V. P. Frolov, *J. High Energy Phys.* **2014**, 049 (2014), https://doi.org/10.1007/JHEP05(2014)049, arXiv:1402.5446 [hep-th].
38. S. G. Ghosh, *Eur. Phys. J. C* **75**, 532 (2015), https://doi.org/10.1140/epjc/s10052-015-3740-y, arXiv:1408.5668 [gr-qc].
39. J. C. S. Neves and A. Saa, *Phys. Lett. B* **734**, 44 (2014), https://doi.org/10.1016/j.physletb.2014.05.026, arXiv:1402.2694 [gr-qc].
40. B. Toshmatov, B. Ahmedov, A. Abdujabbarov and Z. Stuchlik, *Phys. Rev. D* **89**, 104017 (2014), https://doi.org/10.1103/PhysRevD.89.104017, arXiv:1404.6443 [gr-qc].
41. V. K. Tinchev, *Chin. J. Phys.* **53**, 110113 (2015), https://doi.org/10.6122/CJP.20150810, arXiv:1512.09164 [gr-qc].
42. Z.-Y. Fan and X. Wang, *Phys. Rev. D* **94**, 124027 (2016), https://doi.org/10.1103/PhysRevD.94.124027, arXiv:1610.02636 [gr-qc].
43. B. Toshmatov, Z. Stuchlík and B. Ahmedov, *Phys. Rev. D* **95**, 084037 (2017), https://doi.org/10.1103/PhysRevD.95.084037, arXiv:1704.07300 [gr-qc].
44. B. Toshmatov, Z. Stuchlík and B. Ahmedov, Note on the character of the generic rotating charged regular black holes in general relativity coupled to nonlinear electrodynamics, in *Workshop on Black Holes and Neutron Stars*, Opava, Czech Republic (2017), arXiv:1712.04763 [gr-qc].

45. A. Simpson and M. Visser, *J. Cosmol. Astropart. Phys.* **2019**, 042 (2019), https://doi.org/10.1088/1475-7516/2019/02/042, arXiv:1812.07114 [gr-qc].
46. A. Simpson, P. Martin-Moruno and M. Visser, *Class. Quantum Grav.* **36**, 145007 (2019), https://doi.org/10.1088/1361-6382/ab28a5, arXiv:1902.04232 [gr-qc].
47. F. S. N. Lobo, M. E. Rodrigues, M. V. D. S. Silva, A. Simpson and M. Visser, *Phys. Rev. D* **103**, 084052 (2021), https://doi.org/10.1103/PhysRevD.103.084052, arXiv:2009.12057 [gr-qc].
48. A. Simpson and M. Visser, *Universe* **6**, 8 (2019), https://doi.org/10.3390/universe6010008, arXiv:1911.01020 [gr-qc].
49. S. Brahma, C.-Y. Chen and D.-H. Yeom, *Phys. Rev. Lett.* **126**, 181301 (2021), https://doi.org/10.1103/PhysRevLett.126.181301, arXiv:2012.08785 [gr-qc].
50. J. Mazza, E. Franzin and S. Liberati, *J. Cosmol. Astropart. Phys.* **2021**, 082 (2021), https://doi.org/10.1088/1475-7516/2021/04/082.
51. E. Franzin, S. Liberati, J. Mazza, A. Simpson and M. Visser, arXiv:2104.11376 [gr-qc].
52. J. Rayimbaev, B. Narzilloev, A. Abdujabbarov and B. Ahmedov, *Galaxies* **9**, 71 (2021), https://doi.org/10.3390/galaxies9040071.
53. B. Narzilloev, J. Rayimbaev, A. Abdujabbarov and B. Ahmedov, *Galaxies* **9**, 63 (2021), https://doi.org/10.3390/galaxies9030063.
54. B. Narzilloev, S. Shaymatov, I. Hussain, A. Abdujabbarov, B. Ahmedov and C. Bambi, *Eur. Phys. J. C* **81**, 849 (2021), https://doi.org/10.1140/epjc/s10052-021-09617-4, arXiv:2109.02816 [gr-qc].
55. B. Narzilloev, I. Hussain, A. Abdujabbarov, B. Ahmedov and C. Bambi, *Eur. Phys. J. Plus* **136**, 1032 (2021), https://doi.org/10.1140/epjp/s13360-021-02039-x, arXiv:2110.01772 [gr-qc].
56. B. Narzilloev, *J. Fundam. Appl. Res.* **1**, 20210001 (2021).
57. B. Narzilloev, I. Hussain, A. Abdujabbarov and B. Ahmedov, *Eur. Phys. J. Plus* **137**, 645 (2022), https://doi.org/10.1140/epjp/s13360-022-02872-8, arXiv:2205.11760 [gr-qc].
58. B. Narzilloev and B. Ahmedov, *Symmetry* **14**, 1765 (2022), https://doi.org/10.3390/sym14091765.
59. B. Narzilloev and B. Ahmedov, *New Astron.* **98**, 101922 (2023), https://doi.org/10.1016/j.newast.2022.101922.
60. B. Narzilloev, A. Abdujabbarov and A. Hakimov, *Int. J. Mod. Phys. A* **37**, 2250144 (2022), https://doi.org/10.1142/S0217751X22501445.
61. B. Narzilloev and B. Ahmedov, *Symmetry* **15**, 293 (2023), https://doi.org/10.3390/sym15020293.
62. T. Mirzaev, S. Li, B. Narzilloev, I. Hussain, A. Abdujabbarov and B. Ahmedov, *Eur. Phys. J. Plus* **138**, 47 (2023), https://doi.org/10.1140/epjp/s13360-022-03632-4.
63. V. Frolov, P. Krtous and D. Kubiznak, *Living Rev. Relativ.* **20**, 6 (2017), https://doi.org/10.1007/s41114-017-0009-9.
64. B. Carter, *Phys. Rev.* **174**, 1559 (1968), https://doi.org/10.1103/PhysRev.174.1559.
65. B. Carter, *Commun. Math. Phys.* **10**, 280 (1968).
66. A. Simpson and M. Visser, *J. Cosmol. Astropart. Phys.* **2022**, 011 (2022), https://doi.org/10.1088/1475-7516/2022/03/011.
67. I. Banerjee, S. Sau and S. Sengupta, *J. Cosmol. Astropart. Phys.* **2022**, 066 (2022), https://doi.org/10.1088/1475-7516/2022/09/066.
68. S. E. Vazquez and E. P. Esteban, *Nuovo Cim. B* **119**, 489 (2004). arXiv:gr-qc/0308023, https://doi.org/10.1393/ncb/i2004-10121-y.
69. K. Hioki and K.-I. Maeda, *Phys. Rev. D* **80**, 024042 (2009), https://doi.org/10.1103/PhysRevD.80.024042.